Abnormal Coronary Function in Mice Deficient in α_{1H} T-type Ca^{2+} Channels

Chien-Chang Chen,[1,2] Kathryn G. Lamping,[4,5,7]
Daniel W. Nuno,[4,5,7] Rita Barresi,[1,2] Sally J. Prouty,[1,2]
Julie L. Lavoie,[4] Leanne L. Cribbs,[8] Sarah K. England,[2]
Curt D. Sigmund,[4] Robert M. Weiss,[4,7] Roger A. Williamson,[6]
Joseph A. Hill,[9] Kevin P. Campbell[1,2,3]*

Calcium ion (Ca^{2+}) influx through voltage-gated Ca^{2+} channels is important for the regulation of vascular tone. Activation of L-type Ca^{2+} channels initiates muscle contraction; however, the role of T-type Ca^{2+} channels (T-channels) is not clear. We show that mice deficient in the α_{1H} T-type Ca^{2+} channel ($\alpha_1$3.2-null) have constitutively constricted coronary arterioles and focal myocardial fibrosis. Coronary arteries isolated from $\alpha_1$3.2-null arteries showed normal contractile responses, but reduced relaxation in response to acetylcholine and nitroprusside. Furthermore, acute blockade of T-channels with Ni^{2+} prevented relaxation of wild-type coronary arteries. Thus, Ca^{2+} influx through α_{1H} T-type Ca^{2+} channels is essential for normal relaxation of coronary arteries.

Calcium influx through voltage-gated Ca^{2+} channels initiates many physiological events including neurotransmitter release, muscle contraction, and gene expression. Of the voltage-gated calcium channels, the T-type Ca^{2+} channels (Ca$_v$3) that open at lower membrane potential are the least understood. The pore-forming subunits of Ca$_v$3 are encoded by at least three genes: *Cacna1G*, *Cacna1H*, and *Cacna1I* ($\alpha_1$3.1, 3.2, and 3.3, respectively) (*1–3*). $\alpha_1$3.2 is expressed in multiple tissues including brain, heart, liver, testis, zona glomerulosa, skeletal muscle, and spermatids (*2, 4–6*). In the heart, Ca$_v$3 channels are expressed at high density in the sinoatrial (SA) and atrioventricular (AV) nodes (*7, 8*), consistent with a potential role for Ca$_v$3 channels in the generation of pacemaker potentials.

Cardiac Ca$_v$3 channels have been implicated in cardiac hypertrophy. Under normal conditions, T-type Ca^{2+} currents (T-currents) are not expressed in adult ventricular myocytes; however, T-currents can be reexpressed after development of hypertrophy (*9, 10*). In cardiomyopathic BIO 14.6 hamsters, an abnormal increase in T-current density may be responsible for Ca^{2+} overload in the heart (*11*). These studies

suggest that Ca$_v$3 channels may function in the remodeling of cardiac myocytes during development of cardiomyopathy. In smooth muscle, Ca$_v$3 channels may function in vasoconstriction of rat mesenteric arterioles and renal resistance vessels (*12, 13*). Expression of T-currents is regulated during the cell cycle, with the highest density of T-currents during G$_1$ and S phases in smooth muscle and neonatal ventricular myocytes (*14, 15*). Thus, Ca$_v$3 channels appear to take part in signaling pathways that control differentiation and proliferation.

To explore the roles of Ca$_v$3.2, we have generated mice lacking $\alpha_1$3.2 by homologous gene targeting. Homologous recombination resulted in deletion of exon 6, corresponding to amino acid residues 216 to 267 (fig. S1, A and B). Heterozygous mice were bred to generate homozygous mutants ($\alpha_1$3.2$^{-/-}$). Northern blot and Western blot analysis confirmed the loss of $\alpha_1$3.2 RNA and protein in $\alpha_1$3.2$^{-/-}$ mice (fig. S1, C and D). Because $\alpha_1$3.2 is the predominant α_1 subunit of T-channels in rat dorsal root ganglia (DRG) (*16*), we performed whole-cell patch-clamp analysis of voltage-activated Ca^{2+} currents from neonatal DRG neurons. An averaged low voltage–activated Ca^{2+} current (I_T) was elicited by a voltage change from –90 mV to –30 mV (fig. S1E). The peak current density of I_T was –3.7 ± 0.3 pA/pF ($n = 5$) in wild-type DRG neurons. I_T was significantly diminished in the $\alpha_1$3.2$^{-/-}$ DRG neurons ($n = 8$, $P < 0.001$). Thus, $\alpha_1$3.2 channels are the predominant T-channels in neonatal mouse DRG neurons, with no compensation of other $\alpha_1$3 proteins in $\alpha_1$3.2$^{-/-}$ DRG neurons. There were no significant differences between the high voltage–activated (HVA) Ca^{2+} currents

(elicited from –50 mV to 10 mV) from wild-type or $\alpha_1$3.2$^{-/-}$ DRG neurons (fig. S1F). $\alpha_1$3.2$^{-/-}$ mice were viable and fertile. Both male and female $\alpha_1$3.2$^{-/-}$ mice were smaller than their littermate controls. The body weights of 8-week-old male wild-type and $\alpha_1$3.2$^{-/-}$ mice were 26.6 ± 0.92 g ($n = 8$) and 20.2 ± 2.4 g ($n = 9$), respectively (t test, $P < 0.05$). No differences were detected in ratios of specific tissues to total body weight between wild-type and knockout mice.

T-channels are thought to be important in the generation of pacemaker potentials in SA and AV nodes. To investigate whether disruption of $\alpha_1$3.2 produces cardiac abnormalities, we compared hearts isolated from wild-type and $\alpha_1$3.2$^{-/-}$ mice at various ages histologically. Diffuse regions of cardiac fibrosis were observed in ventricular walls from 10-week-old $\alpha_1$3.2$^{-/-}$ mice but not those from wild-type hearts (Fig. 1A). The percentage of cardiac fibrosis area was 0.23 ± 0.06% ($n = 4$) and 2.16 ± 0.57% ($n = 4$) in 10-week-old wild-type and $\alpha_1$3.2$^{-/-}$ hearts, respectively ($P < 0.05$). With increasing age, the size of the fibrotic regions increased. At 1 year of age, the $\alpha_1$3.2$^{-/-}$ hearts had more severe cardiac pathology (Fig. 1B). Large areas of fibrosis, necrosis, and lymphocyte infiltration were observed only in the $\alpha_1$3.2$^{-/-}$ mice. The percentage of cardiac fibrosis area was 0.92 ± 0.3% ($n = 4$) and 4.04 ± 0.89% ($n = 4$) in 1-year-old wild-type and $\alpha_1$3.2$^{-/-}$ hearts, respectively ($P < 0.05$). Electrocardiographic (ECG) telemetry and echocardiography in wild-type and $\alpha_1$3.2$^{-/-}$ mice (fig. S3; movies S1 and S2) showed no significant differences in heart rate between wild-type (565.6 ± 23 beats/min, $n = 16$) and $\alpha_1$3.2$^{-/-}$ mice (505.2 ± 34.7 beats/min, $n = 14$). No cardiac arrhythmias were observed and ECG waveform morphologies were normal. On the other hand, α_{1D} ($\alpha_1$1.3) L-type Ca^{2+} channel–deficient mice have sinus bradycardia and arrhythmia with normal Ca$_v$3 currents in the SA node (*17–19*). Thus, we conclude that even though both T-type and $\alpha_1$1.3 L-type Ca^{2+} channels have the intrinsic ability to support pacemaker activity in the SA node, $\alpha_1$1.3 L-type Ca^{2+} channels contribute more toward the generation of pacemaker potential in the heart.

Because T-channels are not expressed in adult mouse ventricular myocytes, we hypothesized that cardiac fibrosis was due to the loss of $\alpha_1$3.2 in other cells such as vascular smooth muscle. Abnormal coronary artery constriction can lead to reduced coronary blood flow, cardiac myocyte necrosis, and cardiac fibrosis (*20, 21*). Thus, we perfused mice with latex Microfil to visualize the architecture of the coronary tree. In wild-type ($n = 6$) and heterozygous ($n = 3$) hearts, the vessels appeared smooth and regular, but in hearts from $\alpha_1$3.2$^{-/-}$ mice, vessels were con-

[1]Howard Hughes Medical Institute, [2]Department of Physiology and Biophysics, [3]Department of Neurology, [4]Department of Internal Medicine, [5]Department of Pharmacology, [6]Department of Obstetrics and Gynecology, University of Iowa, Iowa City, IA 52242, USA. [7]Veterans Administration Medical Center, Iowa City, IA 52242, USA. [8]Cardiovascular Institute, Loyola University Medical Center, 2160 South First Avenue, Maywood, IL 60153, USA. [9]Division of Cardiology, University of Texas Southwestern Medical Center, Dallas, TX 75390, USA.

*To whom correspondence should be addressed. E-mail: kevin-campbell@uiowa.edu
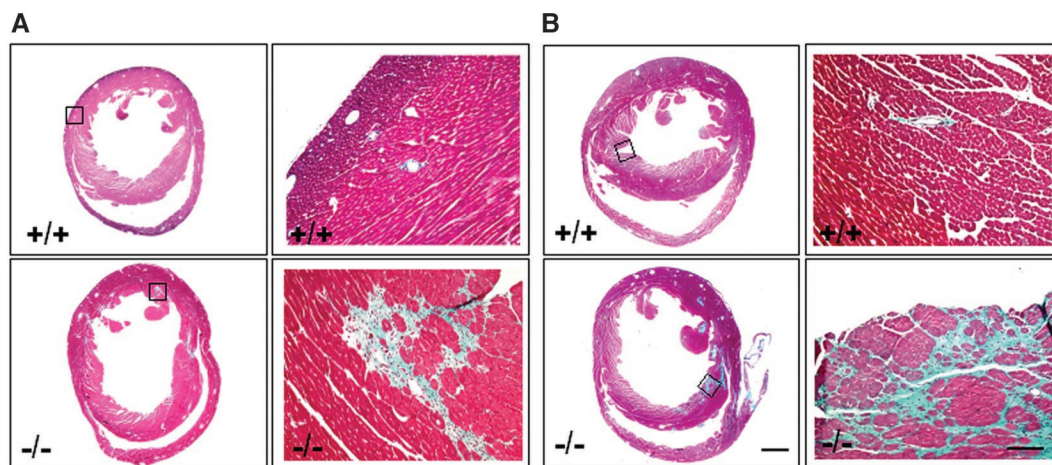
Fig. 1. Cardiac fibrosis and abnormal cardiac vasculature in $\alpha_1 3.2^{-/-}$ mice. (**A**) Masson's trichromic staining of transverse heart sections from 10-week-old wild-type (+/+) and $\alpha_1 3.2^{-/-}$ mice. Regions of cardiac fibrosis are shown in green. (**B**) Larger regions of fibrosis in the $\alpha_1 3.2^{-/-}$ heart at 1 year of age. Scale bar, left panels, 1 mm; right panels, 50 μm. (**C**) Microfil perfusion of coronary arteries in wild-type, heterozygous (+/–), and $\alpha_1 3.2^{-/-}$ hearts. Spiral vascular constrictions are indicated by arrowheads. Scale bar, 40 μm.
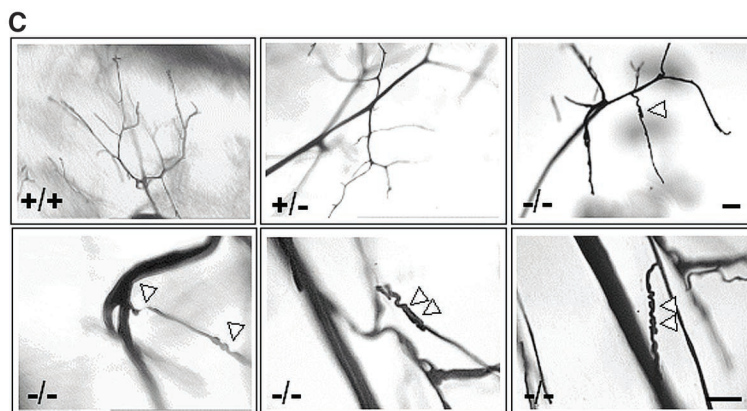
Fig. 2. Impaired relaxation response in the coronary artery of $\alpha_1 3.2^{-/-}$ mice. (**A** to **D**) Percent change in diameter of coronary arteries from wild-type and $\alpha_1 3.2^{-/-}$ mice treated with U46619 (A), ACh (B), SNP (C), and nifedipine (D). In (C), wild-type arteries were also treated with 100 μM Ni^{2+}. (**E**) Blockade of Ca$_v$3 currents with Ni^{2+} decreases ACh-induced (10^{-4} M) relaxation in wild-type arteries.

stricted and had irregular spiral shapes ($n = 10$) (Fig. 1C).

We also measured responses of isolated coronary arteries from wild-type and $\alpha_1 3.2^{-/-}$ hearts. Coronary arteries were isolated, cannulated into micropipettes, and pressurized, and the luminal diameter of the artery was measured with an electronic video dimension analyzer (22). Baseline diameters of coronary arteries from wild-type ($n = 12$) and $\alpha_1 3.2^{-/-}$ mice ($n = 18$) were 103.3 ± 4.5 μm and 112.5 ± 6.7 μm, respectively. U46619, a thromboxane mimetic, produced a similar dose-dependent constriction of coronary arteries from wild-type and $\alpha_1 3.2^{-/-}$ mice (Fig. 2A). Maximal contraction by U46619 was 41 ± 8% ($n = 5$) and 36 ± 11% ($n = 5$) in wild-type and $\alpha_1 3.2^{-/-}$ arteries, respectively.

Similar constriction was observed when KCl was used to constrict arteries from wild-type and $\alpha_1 3.2^{-/-}$ hearts. These data suggest that contractile mechanisms in coronary arteries are normal in the $\alpha_1 3.2^{-/-}$ mice.

We also examined relaxation of coronary arteries in response to acetylcholine (ACh) and sodium nitroprusside (SNP). In arteries from wild-type mice that had been constricted with U46619, ACh produced dose-dependent dilation (Fig. 2B). In contrast, ACh caused further constriction in coronary arteries from $\alpha_1 3.2^{-/-}$ mice. Dilation in response to ACh in mouse coronary arteries is mediated predominantly by release of nitric oxide (NO) from endothelial cells (22). We therefore compared responses of coronary arteries from wild-type and $\alpha_1 3.2^{-/-}$ mice to SNP, an NO donor. SNP induced a dose-dependent dilation of coronary arteries from wild-type mice (Fig. 2C). However, relaxation in response to SNP (10^{-5} M) was reduced to 40 ± 11% ($n = 5$) in arteries from $\alpha_1 3.2^{-/-}$ mice. To ensure that $\alpha_1 3.2^{-/-}$ arteries can relax in response to other dilators, we tested effects of nifedipine (an L-type Ca^{2+} channel blocker). Nifedipine produced similar relaxation of arteries isolated from wild-type ($n = 8$) or $\alpha_1 3.2^{-/-}$ ($n = 5$) mice (Fig. 2D). Thus, only the NO-mediated relaxation appears to be defective in $\alpha_1 3.2^{-/-}$ coronary arteries.

Fig. 3. Expression of $\alpha_1 3.2$ T-type calcium channels in smooth muscle cells. Left panels: Averaged T-currents ($n = 4$) (**A**) and HVA Ca^{2+} currents ($n = 6$) (**B**) recorded from isolated wild-type (+/+) and $\alpha_1 3.2^{-/-}$ coronary smooth muscle cells. Right panels: Peak current density from wild-type and $\alpha_1 3.2^{-/-}$ coronary smooth muscle cell; *$P < 0.001$ (t test).
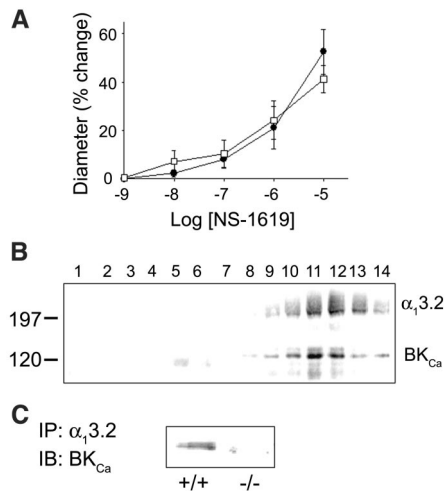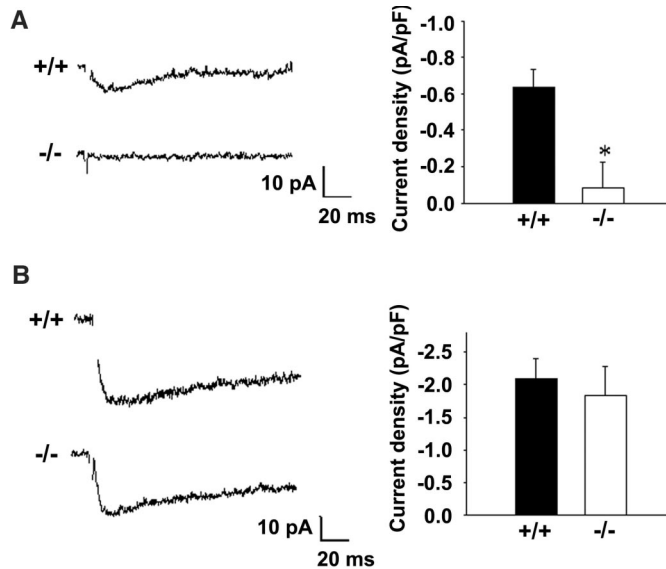

Fig. 4. Association of $\alpha_1 3.2$ T-type calcium channels and α subunit of BK_{Ca} channels. (**A**) Percent change in diameter of coronary arteries from wild-type and $\alpha_1 3.2^{-/-}$ mice treated with NS-1619. (**B**) Western blot analysis of sucrose gradient fractionation of 1% digitonin-solubilized microsomes from HEK cells expressing $\alpha_1 3.2$ and BK_{Ca} channels. (**C**) Coimmunoprecipitation of BK_{Ca} channels with an antibody to $\alpha_1 3.2$ T-type calcium channels from wild-type but not $\alpha_1 3.2^{-/-}$ brain microsomes.

Ca^{2+} influx through Ca^{2+} channels is generally thought to initiate contractile mechanisms in smooth muscle. However, our results suggest that $\alpha_1 3.2$ is required for NO-mediated relaxation. If Ca^{2+} influx through T-channels is required for the relaxation of coronary arteries, blockade of T-channels with Ni^{2+} should decrease relaxation of coronary arteries from wild-type mice. When Ni^{2+} was added in the presence of U46619 and ACh, ACh-induced dilation was decreased in a dose-dependent manner (Fig. 2E).

To determine whether the defect in relaxation is due to altered endothelial cell NO production or abnormal smooth muscle cell function (or both), we compared responses to SNP in the presence and absence of Ni^{2+}. In the presence of 100 μM Ni^{2+}, relaxation of wild-type arteries in response to SNP was reduced to levels similar to those in $\alpha_1 3.2^{-/-}$ arteries (Fig. 2C). These results suggest that Ni^{2+} may affect smooth muscle cells directly rather than through inhibition of endothelial release of NO. We detected T-channels by whole-cell patch-clamp analysis of voltage-activated Ca^{2+} currents on coronary smooth muscle cells isolated from wild-type but not $\alpha_1 3.2^{-/-}$ mice (Fig. 3A). There were no significant differences between the HVA currents from wild-type or $\alpha_1 3.2^{-/-}$ cells (Fig. 3B). Taken together, these results suggest that Ca^{2+} influx through $Ca_v 3.2$ channels in coronary smooth muscle is required for normal relaxation of coronary arteries mediated by endogenously released or exogenously administered NO.

The mechanism underlying the involvement of $\alpha_1 3.2$ in the relaxation of coronary smooth muscle is not clear. Ca^{2+} influx can activate localized calcium release through ryanodine receptors, which in turn activates the large-conductance Ca^{2+}-sensitive K^+ channels (BK_{Ca}), causing an outward K^+ current and membrane hyperpolarization (23, 24). This closes Ca^{2+} channels in the plasma membrane and inhibits contraction. Because BK_{Ca} channels play an important role in regulating relaxation, it is possible that $\alpha_1 3.2$ is functionally coupled to the BK_{Ca} channel in coronary smooth muscle. Deletion of $\alpha_1 3.2$ may reduce the activity of the BK_{Ca} channel, leading to impaired relaxation of coronary arteries. If one of the physiological roles of $\alpha_1 3.2$ is to fine-tune the activity of BK_{Ca} channels in vascular smooth muscle, activation of BK_{Ca} channels should relax constricted $\alpha_1 3.2^{-/-}$ coronary arteries. NS-1619, a BK_{Ca} channel opener, induced similar dose-dependent relaxations of wild-type and $\alpha_1 3.2^{-/-}$ coronary arteries (Fig. 4A). Consistent with possible association of $\alpha_1 3.2$ with the BK_{Ca} channel in vivo, the proteins cosedimented on sucrose gradients when isolated from solubilized human embryonic kidney (HEK) cells overexpressing exogenous $\alpha_1 3.2$ and α subunit of BK_{Ca} channels (Fig. 4B). $\alpha_1 3.2$ and BK_{Ca} channels were also coimmunoprecipitated with an antibody to $\alpha_1 3.2$ from wild-type solubilized brain microsomes but not from $\alpha_1 3.2^{-/-}$ tissues (Fig. 4C).

Our study provides insights into the role of α_{1H} $Ca_v 3$ channels in the normal relaxation of coronary vascular smooth muscle. The results suggest that *Cacna1H* could be a potential target for therapeutic intervention in cardiovascular diseases.

References and Notes
1. E. Perez-Reyes, *J. Bioenerg. Biomembr.* **30**, 313 (1998).
2. L. L. Cribbs *et al.*, *Circ. Res.* **83**, 103 (1998).
3. J. H. Lee *et al.*, *J. Neurosci.* **19**, 1912 (1999).
4. P. Bijlenga *et al.*, *Proc. Natl. Acad. Sci. U.S.A.* **97**, 7627 (2000).
5. A. D. Schrier, H. Wang, E. M. Talley, E. Perez-Reyes, P. Q. Barrett, *Am. J. Physiol. Cell Physiol.* **280**, C265 (2001).
6. W. Y. Son *et al.*, *Dev. Growth Differ.* **44**, 181 (2002).
7. N. Hagiwara, H. Irisawa, M. Kameyama, *J. Physiol.* **395**, 233 (1988).
8. G. Bohn *et al.*, *FEBS Lett.* **481**, 73 (2000).
9. H. B. Nuss, S. R. Houser, *Circ. Res.* **73**, 777 (1993).
10. M. L. Martinez, M. P. Heredia, C. Delgado, *J. Mol. Cell. Cardiol.* **31**, 1617 (1999).
11. L. Sen, T. W. Smith, *Circ. Res.* **75**, 149 (1994).
12. F. Gustafsson, D. Andreasen, M. Salomonsson, B. L. Jensen, N. Holstein-Rathlou, *Am. J. Physiol. Heart Circ. Physiol.* **280**, H582 (2001).
13. P. B. Hansen, B. L. Jensen, D. Andreasen, O. Skott, *Circ. Res.* **89**, 630 (2001).
14. T. Kuga, S. Kobayashi, Y. Hirakawa, H. Kanaide, A. Takeshita, *Circ. Res.* **79**, 14 (1996).
15. W. Guo, K. Kamiya, I. Kodama, J. Toyama, *J. Mol. Cell. Cardiol.* **30**, 1095 (1998).
16. E. M. Talley *et al.*, *J. Neurosci.* **19**, 1895 (1999).
17. J. Platzer *et al.*, *Cell* **102**, 89 (2000).
18. Y. Namkung *et al.*, *J. Clin. Invest.* **108**, 1015 (2001).
19. M. E. Mangoni *et al.*, *Proc. Natl. Acad. Sci. U.S.A.* **100**, 5543 (2003).
20. R. Coral-Vazquez *et al.*, *Cell* **98**, 465 (1999).
21. W. A. Chutkow *et al.*, *J. Clin. Invest.* **110**, 203 (2002).
22. K. G. Lamping, D. W. Nuno, E. G. Shesely, N. Maeda, F. M. Faraci, *Am. J. Physiol. Heart Circ. Physiol.* **279**, H1906 (2000).
23. M. T. Nelson, J. M. Quayle, *Am. J. Physiol.* **268**, C799 (1995).
24. R. Brenner *et al.*, *Nature* **407**, 870 (2000).
25. We thank R. Smith and all members of the Campbell laboratory for critical reading of the manuscript, fruitful discussions, and reagents; A. J. Wilson, K. Garringer, M. Hassebrock, and J. Flanagan for expert technical assistance; Merck & Co. for antibodies; and the University of Iowa DNA core facility for DNA sequencing. Supported by the Donald W. Reynolds Center for Clinical Cardiovascular Research (J.A.H.), NIH and the American Heart Association (K.G.L.), and the Muscular Dystrophy Association (C.-C.C., R.B., K.P.C.). K.P.C. is an investigator of the Howard Hughes Medical Institute.